2019 27th European Signal Processing Conference (EUSIPCO)

Spectral Coexistence of 5G Networks and Satellite Communication Systems Enabled by Coordinated Caching and QoS-Aware Resource Allocation

Konstantinos Ntougias, Constantinos B. Papadias
Athens Information Technology
Athens, Greece
{kontou, cpap}@ait.gr

Georgios K. Papageorgiou
Heriot-Watt University
Edinburgh, UK
g.papageorgiou@hw.ac.uk

Gerhard Hasslinger
Deutsche Telekom
Darmstadt, Germany
gerhard.hasslinger@telekom.de

***Abstract*—The combination of underlay spectrum sharing and coordinated multi-point technologies promises substantial spectral efficiency (SE) gains for 5G cellular networks. In this work, we present a family of simple cooperative mobile edge caching strategies that create joint transmission (JT) opportunities and make use of the non-computational-demanding score-gated least recently used (SG-LRU) caching scheme to achieve high cache hit rate, thus increasing the sum-SE and reducing both the backhaul traffic and the content access latency. In addition, we derive a low-complexity coordinated quality-of-service (QoS) aware resource allocation scheme that maximizes the sum-SE of coordinated beamforming (CBF) under given transmission power per base station, inter-system interference power, and per-user QoS constraints as well as simple alternatives for both CBF and JT. We consider a use case where a cellular network coexists with a fixed satellite service earth station in the 3.7-4.2 GHz C-band. Numerical simulations illustrate the performance gains of the proposed coordinated caching and resource allocation strategies and shed light on the impact of various parameters on their efficiency.**

***Index Terms*—Coordinated Multi-Point (CoMP), cooperative content caching redundancy enhancement (C3RE), score-gated least-recently used (SG-LRU), coordinated QoS-aware interference-constrained PA (CQA-ICPA), interference-constrained equal power allocation (ICEPA).**

I. Introduction

Sub-6 GHz spectrum will play an important role in the 5G landscape. In this regime, the mobile network operators will rely on network densification as well as on technologies that increase the spectral efficiency (SE) [1], to cope with the exponential growth of the mobile data traffic's volume [2].

Underlay spectrum sharing [3] and coordinated multi-point (CoMP) [4] constitute characteristic examples of such technologies. The utilization of CoMP as an enabler of underlay spectrum sharing has the ability to ensure certain quality-of-service (QoS) to the end users and provide substantial SE gains, thanks to the non-orthogonal spectrum access characteristic of underlay spectrum sharing on one hand and the advanced interference management and resource allocation features of CoMP on the other. Given the pivotal role of the C-band in general [5], [6] and the 3.7-4.2 GHz frequency range in particular [7] in 5G mobile broadband access, a possible application of this spectrum sharing paradigm could be, for instance, the facilitation of the harmonious coexistence between 5G cellular networks and fixed satellite service earth stations (FES) that operate in this frequency band, as a replacement of the inefficient approaches of frequency partitioning or spectrum clearing [8]. Nevertheless, this spectrum management model has been largely overlooked in the literature, to our utmost surprise. Furthermore, the few relevant studies consider sum-SE maximization problems and, consequently, propose corresponding resource allocation schemes that are QoS-agnostic (e.g., see [9]).

Coordinated mobile edge caching can create joint transmission (JT) opportunities by increasing the redundancy of the files that are stored in the local caches of the base stations (BS), thus enhancing the sum-SE while eliminating the, otherwise required, data exchanges over the mobile fronthaul (MFH) [10]. At the same time, though, the employed content placement scheme should achieve high cache hit rate by caching the most popular files, so that the traffic on the mobile backhaul (MBH) and the content access latency that are attributed to cache misses are reduced [11]. The small subset of relevant works that consider the joint optimization of the radio access and MBH performance assumes a dense network of overlapping cells and focuses on balancing the redundancy and diversity of the files that are stored in the distributed caches to enable a nearby small-cell BS to serve a user when JT cannot take place [12], [13]. Such uncoordinated transmissions, though, are highly suboptimal from a capacity maximization and interference management point of view, especially under the considered underlay spectrum sharing context. Moreover, the least recently used (LRU) and similar caching strategies that are commonly applied in practice due to their simple implementation, fast cache updates, and ability of adaptation to changes in the access pattern [14], [15] are suboptimal, in terms of the achieved cache hit rate [16], [17].

In this work, we aspire to fill the aforementioned gaps in the literature. More specifically, we consider an underlay spectrum sharing setup where a CoMP-enabled cellular network coexists

This work has been funded by the EC H2020 project BlueSpace (Grant agreement ID: 762055).

978-9-0827-9703-9/19/$31.00 ©2019 IEEE

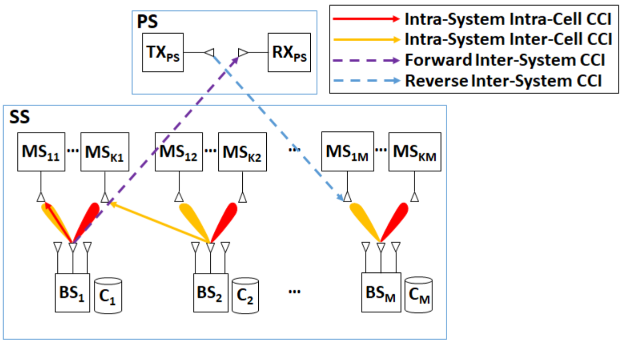

Fig. 1. System setup, notation, and types of interference.

with a FES in the 3.7-4.2 GHz band. We derive a novel low-complexity QoS-aware resource allocation method that maximizes the sum-SE of coordinated beamforming (CBF) while respecting the given transmission and interference power constraints and meeting the per-user QoS requirements, as well as simple QoS-agnostic alternatives for both CBF and JT that relax the sum-SE maximization objective. In addition, we devise a family of simple coordinated caching variants that create JT opportunities to further enhance the sum-SE. The score-gated least recently used (SG-LRU) caching scheme is utilized, an extension of LRU that improves substantially the cache hit rate [17], to reduce the MBH traffic and content access latency. CBF is applied whenever caching-aided JT is not possible. Numerical simulations illustrate the performance gains of the proposed coordinated caching and resource allocation strategies and highlight the effect of various parameters on their efficiency.

II. System Setup and Assumptions

We consider an underlay spectrum sharing setup where the secondary system (SS) is a CoMP-enabled cellular network that adopts universal frequency re-use and the primary system (PS) corresponds to a single-input single-output (SISO) satellite link. We focus on a single cooperation cluster, which is comprised of M cells. In each cell a BS with N antennas and K active single-antenna mobile stations (MS) are located. The m-th BS and the k-th MS in the m-th cell are denoted as BS_m and MS_{km} $(m \in \mathcal{M} = \{1, \dots, M\},\ k \in \mathcal{K} = \{1, \dots, K\})$, whereas the transmitter and the receiver of the PS are denoted as $\mathrm{TX}_{\mathrm{PS}}$ and $\mathrm{RX}_{\mathrm{PS}}$, respectively.

We identify two types of intra-system co-channel interference (CCI), namely, intra-cell multi-user interference (MUI) and inter-cell interference (ICI). Similarly, we identify forward and reverse inter-system (FIS / RIS) CCI created by the transmissions of the BSs and of the PS, respectively.

BS_m is equipped with a local cache C_m that has a storage capacity of C files. The content catalog contains F files $\mathcal{O} = \{O_1, \dots, O_F\}$.

A schematic representation of the system setup, along with the types of interference and the notation, is depicted in Fig. 1.

We consider ideal MFH and MBH, quasi-static frequency-flat Rayleigh fading channels in the terrestrial segment, i.i.d. zero-mean additive white Gaussian noise with unit variance, and availability of perfect channel state information (CSI) at all nodes. Also, we assume that the BSs are informed about the interference power threshold (IPT). Furthermore, we assume i.i.d. Zipf distributed user requests to files with slowly varying popularity [16], [18], [19].

III. System Model and Problem Formulation

A. Notation

The channel between MS_{km} and $\mathrm{TX}_{\mathrm{PS}}$ is denoted as h_{km}, whereas the channel between $\mathrm{RX}_{\mathrm{PS}}$ and $\mathrm{TX}_{\mathrm{PS}}$ is denoted as g $(k \in \mathcal{K},\ m \in \mathcal{M})$. Similarly, the channel between MS_{km} and BS_j is denoted as $\mathbf{h}^j_{km}$, while the channel between $\mathrm{RX}_{\mathrm{PS}}$ and BS_j is denoted as $\mathbf{g}_j$ $(j \in \mathcal{M})$. The BF vector used by BS_j to serve MS_{km}, the power allocated by BS_j to MS_{km}, the data symbol transmitted by BS_j to MS_{km}, and the AWGN at MS_{km} are denoted as $\mathbf{w}^j_{mk}$, P^j_{mk}, s^j_{mk}, and n_{km}, respectively, whereas the transmission power of $\mathrm{TX}_{\mathrm{PS}}$, the data symbol transmitted by $\mathrm{TX}_{\mathrm{PS}}$ to $\mathrm{RX}_{\mathrm{PS}}$, and the AWGN at $\mathrm{RX}_{\mathrm{PS}}$ are denoted as P, d, and z, respectively.

B. System Model

Let us assume that CBF is applied in the SS. We define for $m,\ j \in \mathcal{M}$ and $k \in \mathcal{K}$:

$$\mathbf{v}^j_{mk} = \mathbf{w}^j_{mk} \sqrt{P^j_{mk}} s^j_{mk}. \tag{1}$$

Then, the complex baseband representation of the received signal at MS_{km} is given by:

$$\begin{aligned} y_{km} = {} & \left(\mathbf{h}^m_{km}\right)^\dagger \mathbf{v}^m_{mk} + \sum_{\substack{i=1 \\ i \neq k}}^{K} \left(\mathbf{h}^m_{km}\right)^\dagger \mathbf{v}^m_{mi} \\ & + \sum_{\substack{j=1 \\ j \neq m}}^{M} \sum_{i=1}^{K} \left(\mathbf{h}^j_{km}\right)^\dagger \mathbf{v}^j_{ji} + h_{km}\sqrt{P}d + n_{km}. \end{aligned} \tag{2}$$

The terms in the right-hand side (RHS) of Eq. (2) are, in order, the useful signal component, the intra-cell MUI, the ICI, the RIS CCI, and the AWGN. Note that in CBF $\mathbf{w}^j_{mk} = \mathbf{0}$, $P^j_{mk} = 0$, and $s^j_{mk} = 0$ for $j \neq m$.

The composite signal model, ignoring the RIS CCI for convenience, is given by:

$$\mathbf{y} = \mathbf{H}\mathbf{W}\mathbf{P}^{1/2}\mathbf{s} + \mathbf{n}, \tag{3}$$

where $\mathbf{y}$, $\mathbf{s}$, and $\mathbf{n}$ are the received symbols vector, transmitted symbols vector, and AWGN vector, respectively, whereas $\mathbf{H}$, $\mathbf{W}$, and $\mathbf{P}$ are the composite channel matrix, precoding matrix, and power allocation (PA) matrix, respectively.

The received signal at $\mathrm{RX}_{\mathrm{PS}}$ is given by:

$$y = g\sqrt{P}d + \sum_{m=1}^{M} \sum_{k=1}^{K} \left(\mathbf{g}_m\right)^\dagger \mathbf{w}^m_{mk} \sqrt{P^m_{mk}} s^m_{mk} + z. \tag{4}$$

The terms in the RHS of Eq. (4) are, in order, the useful signal component, the FIS CCI, and the AWGN.

By applying zero-forcing (ZF) precoding at the cellular network in a spectrum-sharing-agnostic manner (i.e., by ignoring all types of inter-system CCI), we eliminate the intra-system CCI (i.e., the intra-cell MUI and the ICI) [4]. The ZF precoding matrix is given by [4]:

$$\mathbf{W}^{(\mathrm{ZF})} = \mathbf{H}^{\#} = \mathbf{H}^{\dagger}\left(\mathbf{H}\mathbf{H}^{\dagger}\right)^{-1}. \tag{5}$$

Notice that the effective channel matrix after precoding, $\overline{\mathbf{H}} = \mathbf{H}\mathbf{W}^{(\mathrm{ZF})}$, is diagonal.

After the application of ZF precoding, the signal-to-interference-plus-noise-ratio (SINR) of MS_{km} is given by:

$$\gamma_{km} = \frac{\left|\left(\mathbf{h}_{km}^{m}\right)^{\dagger}\left(\mathbf{w}_{mk}^{m}\right)^{(\mathrm{ZF})}\right|^{2} P_{mk}^{m}}{\left|h_{km}\right|^{2} P + 1}. \tag{6}$$

The data rate of MS_{km} is given by:

$$R_{km} = \log_2(1+\gamma_{km}) = \log_2(1+\lambda_{mk}^{m} P_{mk}^{m}), \tag{7}$$

where $\lambda_{mk}^{m} = \gamma_{km}/P_{mk}^{m}$.

The sum-rate (SR) throughput of the SS is given by:

$$R = \sum_{m=1}^{M}\sum_{k=1}^{K} R_{km} = \sum_{m=1}^{M}\sum_{k=1}^{K} \log_2(1+\lambda_{mk}^{m} P_{mk}^{m}). \tag{8}$$

C. Problem Formulation

Our goal is to determine the PA scheme that maximizes the SR throughput for the given ZF precoders under a number of transmission and per-user QoS constraints. This optimization problem, which we call $\mathbf{P}$, takes the following form:

$$\min_{\substack{P_{mk}^{m} \\ m\in\mathcal{M},\, k\in\mathcal{K}}} \quad -R = -\sum_{m=1}^{M}\sum_{k=1}^{K} \log_2\left(1+\lambda_{mk}^{m} P_{mk}^{m}\right) \tag{9a}$$

s.t.

$$P_{mk}^{m} \geq 0, \quad m\in\mathcal{M};\ k\in\mathcal{K}, \tag{9b}$$

$$\sum_{k=1}^{K} P_{mk}^{m} \leq P_T, \quad m\in\mathcal{M}, \tag{9c}$$

$$\sum_{m=1}^{M}\sum_{k=1}^{K} \alpha_{mk}^{m} P_{mk}^{m} \leq P_I, \tag{9d}$$

$$\gamma_{km} \geq \tilde{\gamma}_{km}, \quad k\in\mathcal{K},\ m\in\mathcal{M}, \tag{9e}$$

where

$$\alpha_{mk}^{j} = \left|\left(\mathbf{g}_j\right)^{\dagger}\left(\mathbf{w}_{mk}^{j}\right)^{(\mathrm{ZF})}\right|^{2}. \tag{10}$$

Eq. (9b) represents the non-negative transmission power constraints; Eq. (9c) corresponds to the sum-power constraints (SPC) (one per BS); Eq. (9d) refers to the interference power constraint (IPC); and Eq. (9e) expresses the per-user QoS constraints, which state that the provision of a minimum data rate or, equivalently, SINR level should be guaranteed for each user. Such minimum data rate requirements are justified, for instance, by the demand of ensuring video streaming with a baseline video quality [20]. This PA task is convex, thanks to the application of ZF precoding which nulls the coupled interference components in the SINR [4].

Algorithm 1 CQA-ICPA Algorithm for CBF

procedure CQA-ICPA($\lambda_{mk}^{m}, \alpha_{mk}^{m}, P_T, P_I, \tilde{P}_{mk}^{m}$)
  Initialize: $\mu_{\min}$, $\mu_{\max}$
  while $|\mu_{\max} - \mu_{\min}| > \delta_{\mu}$ **do**
    $\mu = (\mu_{\min} + \mu_{\max})/2$
    for $m = 1$ to M **do**
      Find $\min(\nu_m)$, $\nu_m \geq 0$:
      $\sum_{k=1}^{K}\left(\left(\frac{1}{\ln 2(\nu_m+\mu\alpha_{mk}^{m})} - \frac{1}{\lambda_{mk}^{m}} - \tilde{P}_{mk}^{m}\right)^{+} + \tilde{P}_{mk}^{m}\right) \leq P_T$
    end for
    Compute P_{mk}^{m} according to Eq. (11)
    if $\sum_{m=1}^{M}\sum_{k=1}^{K} \alpha_{mk}^{m} P_{mk}^{m} \geq P_I$ **then**
      $\mu_{\min} = \mu$
    else
      $\mu_{\max} = \mu$
    end if
  end while
  Output: P_{mk}^{m}, $m\in\mathcal{M};\ k\in\mathcal{K}$
end procedure

IV. Coordinated Resource Allocation

A. Coordinated Beamforming

The solution of $\mathbf{P}$ is a multi-level water-filling (WF) scheme that is presented in the following theorem [21].

Theorem 1: The solution to $\mathbf{P}$ is given by the coordinated QoS-aware interference-constrained PA (CQA-ICPA) scheme:

$$P_{mk}^{m} = \left(\frac{1}{\ln 2\left(\nu_m + \mu\alpha_{mk}^{m}\right)} - \frac{1}{\lambda_{mk}^{m}} - \tilde{P}_{mk}^{m}\right)^{+} + \tilde{P}_{mk}^{m}, \tag{11}$$

where ν_m and μ are Lagrange multipliers and $\tilde{P}_{mk}^{m}$ is the power that corresponds to $\tilde{\gamma}_{km}$.

The proof of Theorem 1 is obtained by taking the Lagrangian form of $\mathbf{P}$ and applying the Karush-Kuhn-Tucker (KKT) conditions. The iterative algorithm that calculates the Lagrange multipliers and implements the solution of Eq. (11) is presented in Algorithm 1. The algorithm chooses an initial value of μ, calculates the minimum values of ν_m for this value such that the SPCs are met, computes the power levels for the given values of the Lagrange multipliers according to Eq. (11), and then makes use of the bisection method to update the value of μ based on whether the IPC is met or not. The parameter $\delta_{\mu} > 0$ controls the accuracy of the algorithm. Note that when the IPC is inactive, $\mu = 0$ and the algorithm reduces to the corresponding interference-unconstrained solution.

A simple suboptimal alternative resource allocation method would be to ignore the sum-SE maximization objective and the per-user QoS requirements and assign equal power levels to the users, taking though into account the IPC.

Proposition 1: The interference-constrained equal PA (ICEPA) scheme for CBF assigns the following power level to the users:

$$P_c = \min\left(\frac{P_T}{K}, \frac{P_I}{\sum_{m=1}^{M}\sum_{k=1}^{K}\alpha_{mk}^{m}}\right). \tag{12}$$

B. Joint Transmission

The system model for the JT case is similar to the one presented in Section III for CBF, although there are subtle differences attributed to the fact that in this scenario each BS serves all the users of the cluster. We consider the aforementioned suboptimal ICEPA method, adapted to JT:

Proposition 2: The ICEPA scheme for JT assigns to the users the power levels:

$$P_c = \min\left(\frac{P_T}{MK}, \frac{P_I}{\sum_{j=1}^{M}\sum_{m=1}^{M}\sum_{k=1}^{K}\alpha_{mk}^{j}}\right). \tag{13}$$

V. Coordinated Caching

A. Score-Gated LRU

SG-LRU combines an LRU cache, for simple implementation in software as a stack and fast cache updates by placing the requested file on the top of the LRU stack, with a score-gate function that exploits request frequency statistics and incorporates an aging mechanism to gather the most popular files in a recent timeframe in the cache, so that the polution of the cache storage with formerly "hot" but currently irrelevant files is avoided and the cache hit rate is significantly improved [17]. After a cache miss, the requested file enters a SG-LRU cache only if its score is at least equal to the score of the LRU cached file [17]. We consider a sliding window least frequently used (SW-LFU) score-gate function, which restricts request counts in a sliding window and approaches LRU / LFU for small / large window size [16].

B. C3RE Method

The proposed cooperative content caching redundancy enhancement (C3RE) method is described as follows: If the requested file is not found in the target cache (local cache miss), the request is transferred to the other caches of the cluster. In case of a global cache hit, the corresponding remote cache may update only its sliding window (variant A), or both its sliding window and its local storage (variant B), or none of them (variant C), assuming that SG-LRU is utilized (or it may or may not update its local storage, when LRU is utilized instead). Note that whenever a file enters the target cache, the corresponding BS updates both its sliding window and local storage. Clearly this method increases the redundancy of the cached files, thus creating JT opportunities.

VI. Performance Evaluation

In this section, we evaluate the performance of the proposed techniques via numerical simulations. Initially, we study the performance of the considered C3RE variants when SG-LRU is applied versus their performance when LRU is utilized, in terms of the achieved local, global, and total cache hit rate (L-HR, G-HR, and T-HR, respectively). We consider a scenario where there are $M = 5$ caches, each with a storage capacity of $C = 20$ files; the catalog has a size of $F = 1,000$ files; $100,000$ user requests are generated; and the size of the sliding window is $W = 10,000$ requests. In the first use case, the Zipf exponent varies as $\beta = \{0.5, 0.75, 0.99\}$. In the second use case, we fix $\beta = 0.75$ and we vary the cache size as $C = \{2, 20, 200\}$. In the third use case, we fix $C = 20$ and we vary the sliding window size as $W = \{100, 1000, 10000\}$. We note in Fig. 2 that irrespective of the coordinated caching variant, SG-LRU achieves high L-HR and low G-HR, while LRU resembles this behavior when the Zipf exponent has a large value (since then temporal locality provides indirect file popularity information) or the cache size is large and the exact opposite behavior otherwise. The T-HR of both caching schemes is comparable. In both cases, the L-HR gain of SG-LRU over LRU is similar to the single-cache scenario (i.e., $> 10\%$ for large Zipf exponents or caches [17]). Thus, SG-LRU further reduces the cooperation overhead and content access latency. We also notice that a moderate sliding window results in higher T-HR, since in this case the request frequency and recency information is exploited more efficiently towards a representative ranking of the files. In addition, we note that the performance of both caching schemes improves for larger Zipf exponents or caches, as expected.

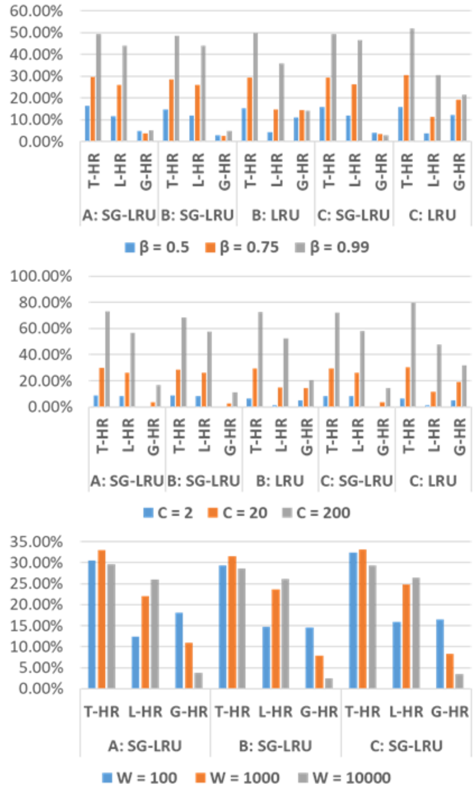

Fig. 2. C3RE variants: SG-LRU vs. LRU. Upper row: Varying Zipf exponent. Middle row: Varying cache size. Lower row: Varying sliding-window size.

Fig. 3 depicts the average sum-SE that is achieved by CBF when either CQA-ICPA or ICEPA is utilized versus the one achieved by C3RE-SG-LRU-aided hybrid CBF / JT with CQA-ICPA / ICEPA for IPT $P_I = 30$ dB or $P_I = 20$ dB over a range of average receive SNR $\overline{\gamma}$ of 0-30 dB in a setup with

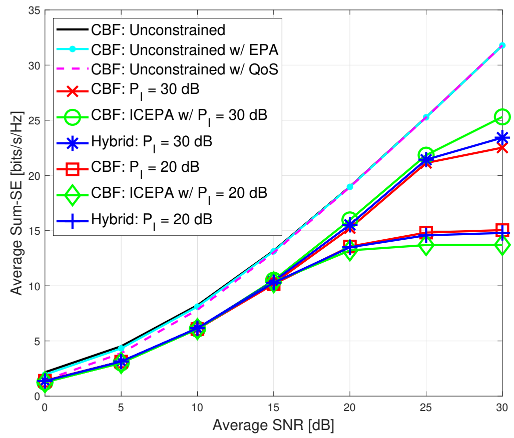

Fig. 3. Sum-SE vs. SNR of CBF vs. CBF / JT hybrid enabled by C3RE with SG-LRU.

$M = 2$ and $K = 2$. The incumbent is a satellite link, the operating spectrum is 3.7-4.2 GHz, and the QoS requirements of the $MK = 4$ users are $\begin{bmatrix} 0.10 & 0.15 & 0.20 & 0.10 \end{bmatrix} \overline{\gamma}$. The power of the RIS CCI at each MS is around 0 dB. The catalog contains $F = 1,000$ files, each cache has size of $C = 20$ files, and the Zipf exponent is $\beta = 0.75$. For comparison purposes, we illustrate also the performance that is achieved in CBF-only mode of operation when the IPC is inactive and the QoS constraints are active ($\mu = 0$ in Eq. (11)) or they are inactive and either optimal, in the sum-SE sense, PA (standard WF-PA scheme [21]) or equal power allocation $P_c = P_T/K$ is applied. We notice that the performance of the CBF-only interference-unconstrained variants converges in the high-SNR regime, while in the low-SNR regime equal power allocation outperforms slightly the QoS-constrained variant. We also note that the performance penalty that is attributed to the requirement of meeting the IPC is greater for more stringent IPTs. Large IPT values result eventually in the flooring of the sum-SE (i.e., the performance does not improve with the SNR). Moreover, in CBF-only mode ICEPA outperforms CQA-ICPA in the high SNR regime when the IPT is tight, while for more relaxed IPTs the situation is reversed. In both cases, the hybrid CBF / JT scheme lies in between these two extremes and is very close to the corresponding CQA-ICPA curve.

VII. Summary and Conclusions

In this paper, we propose a spectrum sharing paradigm that has the ability to increase the sum-SE of 5G networks, reduce the traffic on the MBH and the content access latency, and provide a minimum guaranteed data rate to the end users. To this end, we derived a family of coordinated caching and resource allocation schemes. We evaluated the performance of this system via numerical simulations for a use case where the cellular network coexists with a FES. The simulation results revealed that it is possible to meet both the IPC of an incumbent and the QoS requirements of the mobile users, along with the transmission power constraints. However, for tight IPCs the performance deteriorates quickly. We believe that this work could serve as a first step towards more efficient paradigms of coexistence between 5G cellular networks and satellite communication systems.

References

[1] E. Bjornson, J. Hoydis, and L. Sanguinetti, “Massive MIMO Networks: Spectral, Energy, and Hardware Efficiency,” *Foundations and Trends in Signal Processing*, vol. 11, no. 3-4, pp. 154–655, Nov. 2017.

[2] Cisco, “Cisco Visual Networking Index: Global Mobile Data Traffic Forecast Update, 2016–2021,” White Paper, Mar. 2017.

[3] S. Pandit and G. Singh, “An Overview of Spectrum Sharing Techniques in Cognitive Radio Communication System,” *Wireless Networks*, vol. 23, no. 2, pp. 497–518, Feb. 2017.

[4] E. Bjornson and E. Jorswieck, “Optimal Resource Allocation in Coordinated Multi-Cell Systems,” *Foundations and Trends in Communications and Information Theory*, vol. 9, no. 2-3, pp. 113–381, Jan. 2013.

[5] W. Xiang, K. Zheng, and X. Shen, Eds., *5G Mobile Communications*. Springer, 2017.

[6] M. D. Mueck, S. Srikanteswara, and B. Badic, “Spectrum Sharing: Licensed Shared Access (LSA) and Spectrum Access System (SAS),” Intel, White Paper, Oct. 2015.

[7] “Expanding Flexible Use in Mid-Band Spectrum Between 3.7 and 24 GHz,” FCC, Tech. Rep., Aug. 2017.

[8] G. Hattab *et al.*, “Interference Analysis of the Coexistence of 5G Cellular Networks with Satellite Earth Stations in 3.7-4.2GHz,” in *IEEE International Conference on Communications (ICC)*, Kansas City, MO, USA, May 2018.

[9] D. Denkovski *et al.*, “Generic Multiuser Coordinated Beamforming for Underlay Spectrum Sharing,” *IEEE Transactions on Communications*, vol. 64, no. 6, pp. 2285–2298, Jun. 2016.

[10] F. Zhou *et al.*, “A Cache-Aided Communication Scheme for Downlink Coordinated Multipoint Transmission,” *IEEE Access*, vol. 6, pp. 1416–1427, Dec. 2017.

[11] K. Shanmugam *et al.*, “Femtocaching: Wireless Video Content Delivery Through Distributed Caching Helpers,” *IEEE Transactions on Information Theory*, vol. 59, no. 12, pp. 8402–8413, Dec. 2013.

[12] A. Tuholukova *et al.*, “Optimal Cache Allocation for Femto Helpers with Joint Transmission Capabilities,” in *IEEE International Conference on Communications (ICC)*, Paris, France, May 2017.

[13] W. C. Ao and K. Psounis, “Fast Content Delivery via Distributed Caching and Small Cell Cooperation,” *IEEE Transactions on Mobile Computing*, vol. 17, no. 5, pp. 1048–1061, May 2017.

[14] A. Giovanidis and A. Avranas. (2016) Spatial Multi-LRU: Distributed Caching for Wireless Networks with Coverage Overlaps. [Online]. Available: https://arxiv.org/abs/1612.04363

[15] E. Leonarndi and G. Neglia, “Implicit Coordination of Caches in Small Cell Networks Under Unknown Popularity Profiles,” *IEEE Journal on Selected Areas in Communications*, vol. 36, no. 6, pp. 1276–1285, Jun. 2018.

[16] G. Hasslinger and K. Ntougias, “Evaluation of Caching Strategies Based on Access Statistics of Past Requests,” in *17th International GI/ITG MMB and DFT Conference*, ser. Lecture Notes in Computer Science (LNCS), Springer, Ed., vol. 8376, Bamberg, Germany, Mar. 2014, pp. 120–135.

[17] G. Hasslinger *et al.*, “Performance Evaluation for New Web Caching Strategies Combining LRU with Score Based Object Selection,” *Computer Networks*, vol. 125, pp. 172–186, Oct. 2017.

[18] M. Torteli *et al.*, “Modelgraft: Accurate, Scalable, and Flexible Performance Evaluation of General Cache Networks,” in *International Teletraffic Congress (ITC)*, Wuerzburg, Germany, Sep. 2016.

[19] T. Qiu *et al.*, “Modeling Channel Popularity Dynamics in a Large IPTV System,” in *SIGMETRICS International Joint Conference on Measurement and Modeling of Computer Systems*, Seattle, WA, USA, Jun. 2009, pp. 275–286.

[20] H. Huang *et al.*, Eds., *MIMO Communication for Cellular Networks*. Springer-Verlag New York, 2012.

[21] K. Ntougias *et al.*, “Simple Cooperative Transmission Schemes for Underlay Spectrum Sharing Using Symbol-Level Precoding and Load-Controlled Arrays,” in *International Conference on Acoustics, Speech, and Signal Processing (ICASSP)*, May 2019.